CAAI Transactions on Intelligence Technology

WILEY

ORIGINAL RESEARCH OPEN ACCESS

Distributed *k*-WTA Network for Multi-Manipulator Competition With Experimental Verifications

Shengkai Sun[1,2] | Yutong Li[1,3] | Jianfeng Lv[1]

[1]The School of Information Science and Engineering, Lanzhou University, Lanzhou, China | [2]Gansu Zhonglan Chuanggong Information Technology Co. Ltd., Jinchang, China | [3]School of Astronautics, Harbin Institute of Technology, Harbin, China

Correspondence: Jianfeng Lv (ljf@lzu.edu.cn) | Yutong Li (25B904023@stu.hit.edu.cn)

Received: 18 April 2026 | **Revised:** 3 June 2026 | **Accepted:** 24 June 2026

Keywords: *k*-winner-take-all (*k*-WTA) network | laplacian matrix | multiple-manipulator coordination | noise-suppressing neural dynamics (NSND)

ABSTRACT

In this article, a new distributed *k*-winner-take-all (D*k*-WTA) network is designed and used to construct a dynamic allocation scheme for competitive coordination tasks of multiple manipulators as embodied agents. The scheme is constructed based on the following two aspects. On one hand, with reference to a perspective that the Laplacian matrix is introduced into a *k*-WTA network, a quadratic programming (QP) problem used for the competitive coordination of multiple manipulators is designed. Then, inspired by a noise-suppressing neural dynamics (NSND) method, a D*k*-WTA network is established by solving this QP problem. On the other hand, combined with the forward kinematics, a D*k*-WTA dynamic allocation scheme is constructed. In addition, theoretical analyses on the constructed scheme are conducted regarding convergence and robustness. Finally, for verification of the feasibility of the proposed D*k*-WTA network, simulations and experiments based on multiple manipulators for trajectory-tracking tasks are conducted. Notably, the proposed scheme has the potential to be extended to other embodied multi-agent systems.

1 | Introduction

The *k*-winner-take-all (*k*-WTA) network is a competitive network in which the *k* maximum values can be identified from multiple inputs. Such networks find extensive application across multiple domains, including image processing [1], pattern recognition [2], computational sociology [3], and embodied multi-agent systems [4]. The concept of a *k*-WTA network was first introduced in [5]. Then, a set of integrated circuits is created for executing the function of *k*-WTA. A continuous-time Hopfield *k*-WTA network is constructed, and demonstrated through rigorous theoretical analyses that it can effectively identify the *k* largest components of a sequence [6]. Then, a discrete-time *k*-WTA model with a corresponding circuit scheme is presented in [7]. Subsequently, a *k*-WTA network with continuous-time dynamics is designed in [8], which provides corresponding applications in areas such as the parallel sorting.

Furthermore, for optimising the model structure, the *k*-WTA operation is firstly described as a quadratic programming (QP) problem [9]. Then, an improved dual neural network is used to conduct the *k*-WTA operation by solving a QP problem [10]. In [11, 12], the effect of different noise on this network is analysed. Meanwhile, on the basis of this QP problem, an allocation and control scheme which is used for multi-agent coordination target tracking is presented in [13]. In particular, distributed *k*-WTA networks (D*k*-WTA) are expected to be applied to multi-agent systems to remove the control centre and reduce the communication burden, where every agent merely relies on

This is an open access article under the terms of the Creative Commons Attribution License, which permits use, distribution and reproduction in any medium, provided the original work is properly cited.

© 2026 The Author(s). *CAAI Transactions on Intelligence Technology* published by John Wiley & Sons Ltd on behalf of The Institution of Engineering and Technology and Chongqing University of Technology.

https://doi.org/10.1049/cit2.70164

local data from itself and its nearby nodes within the topological domain. However, the above-mentioned k-WTA networks are depicted in a centralised form, implying that distributed topological constraints are overlooked, making them unsuitable for direct application in multi-agent systems where distributed communication is required [14, 15].

In recent years, numerous Dk-WTA networks have been presented [16]. With the help of a consensus estimator constructed in [17], a Dk-WTA network is obtained [18]. Two state variables for each agent to solve a Dk-WTA problem are introduced in [19]. A consensus-based approach is adopted to construct a distributed network, and the inertia terms are introduced to accelerate the convergence in [20]. In [21], inspired by [19], a Dk-WTA network with a high-pass consensus estimator is designed, and relevant theoretical analyses are fully provided. However, note that in some practical application scenarios, such as multi-agent coordination, the states and information of systems change over time [22]. The above Dk-WTA networks do not take this into account when they are constructed, so lagging errors [23, 24, 25] are inevitable in these networks. Moreover, in practice, there is a non-negligible noise problem, which may seriously affect the performance of a Dk-WTA network when it works. This problem is also overlooked in the above networks. In fact, much literature has focused on competitive coordination of multiple agents based on k-WTA networks, which is different from coordination based on cooperative behaviours [26, 27, 28] and focuses on the mechanism of preferential task allocation to reduce the cost of resources. In particular, lagging errors and noise interference have been studied as two important factors that cannot be ignored. Specifically, in [29], a centralised k-WTA network without lagging errors is constructed. Subsequently, based on it, a centralised k-WTA network considering noise interference is designed in [30]. Although the above studies [29, 30] have made some progress in solving the lagging error problem and the noise problem, they are difficult to be distributed due to the use of the nonlinear complementary penalty (NCP) function to tackle inequality constraints. Meanwhile, note that most of the existing Dk-WTA networks are implemented by introducing a consensus estimator [18–21]. It means that when we focus on lagging errors and noise interference faced by a k-WTA network, the convergence performance and anti-interference ability of the consensus estimator should also be taken into account, which makes the problems more complicated. Hence, it is difficult to directly extend the centralised k-WTA networks [29, 30] mentioned above to distributed ones. Overall, how to construct a Dk-WTA network without lagging errors and considering noise interference is still worth studying. It is worth pointing out that in [31], a Dk-WTA network without the consensus estimator is constructed by introducing a Laplacian matrix to improve the traditional k-WTA problem in the QP form. Although it provides a new idea for the construction of Dk-WTA networks, it faces the problems of lagging errors and noise interference. In addition, all the aforementioned works treat each agent as a point mass, but fails to consider that each agent is embodied in practical application scenarios and do not further incorporate the kinematics of the agents [32, 33, 34]. In view of the above discussions, in this article, a k-WTA problem in the QP form applied to competitive coordination of multiple manipulators is designed. Then, by introducing a noise-suppressing neural dynamics (NSND) method [35], a Dk-WTA network considering both lagging errors and noise interference is constructed, which does not require the consensus estimator. Furthermore, combined with the forward kinematics, a Dk-WTA dynamic allocation scheme is built. To summarise, this article offers the following key contributions.

1. A distributed k-winner-take-all (Dk-WTA) network is built without needing a consensus estimator. Theoretical analyses and numerical comparisons show that this network can resist noise and eliminate lagging errors.
2. By combining forward kinematics, a Dk-WTA based dynamic allocation scheme is developed for multiple manipulators. Using this scheme, a trajectory-tracking task with eight UR5 manipulators is simulated on Matlab and CoppeliaSim. To further test its feasibility, a similar task is carried out on four KINOVA Gen3 lite manipulators in a real experiment.

In addition, the rest of this paper contains four sections. Section 2 formulates the QP-form k-WTA problem and demonstrates the development of the proposed Dk-WTA network along with the corresponding task allocation scheme. Section 3 proves the convergence of the proposed Dk-WTA network in the absence and presence of noise and the equivalence of the constraints between the k-WTA problem used in this article and a classical one. Section 4 shows simulations of a trajectory-tracking task performed by eight UR5 manipulators and analyzes the simulation results. Moreover, experiments based on a multi-manipulator platform with four KINOVA Gen3 lite manipulators are conducted. Section 5 concludes this article. Table 1 summarises the meanings of the mathematical symbols used in the paper. The general structure is depicted in Figure 1.

2 | Problem Formulation and Scheme Design

In this section, a QP problem with equality constraints which describes the k-WTA operation is given according to the new perspective in [31]. Meanwhile, a Dk-WTA network is obtained by solving the QP-form k-WTA problem. In addition, combined with the forward kinematics, a Dk-WTA scheme for multiple manipulators is constructed.

2.1 | Graph Theory

For an n-node topology, the adjacency matrix $\mathbb{A}$ characterises node connections. In an undirected graph, $\mathbb{N}(i)$ denotes the neighbour set of node i. For off-diagonal entries with $i \neq j$, $a_{ij} = a_{ji} = 1$ if $j \in \mathbb{N}(i)$, and 0 otherwise. Diagonal entries satisfy $a_{ii} = 0$.

In particular, the Laplacian matrix is given by $L = \Lambda(\mathbb{A}\mathbf{1}) - \mathbb{A}$ with $\Lambda(\cdot)$ representing the diagonal operation and $\mathbf{1}$ consisting of ones. Furthermore, according to the definition of $\mathbb{A}$ and L, the Laplacian matrix associated with an undirected graph possesses the following characteristics: $L = L^{\mathrm{T}}$ and $L\mathbf{1} = \mathbf{1}^{\mathrm{T}}L = \mathbf{0}$ with superscript T being the transpose symbol.

2.2 | Problem Formulation

The k-WTA operation can be expressed in a mathematical form:

$$\boldsymbol{x}_i(t) = \psi(\boldsymbol{u}_i(t)) = \begin{cases} 1, & \text{if } \boldsymbol{u}_i(t) \in \{k \text{ largest values of } \boldsymbol{u}(t)\}, \\ 0, & \text{otherwise}, \end{cases} \tag{1}$$

where $\psi(\cdot)$ is a mapping function.

TABLE 1 | Meanings of mathematical symbols.

n	The number of nodes in an undirected graph
k	The number of winners
$\mathbb{A} \in \mathbb{R}^{n\times n}$	The adjacency matrix of an undirected graph
$\Lambda(\cdot)$	The diagonal operation
$\mathbf{1} \in \mathbb{R}^n$	A vector consisting of ones
$\mathbf{0} \in \mathbb{R}^n$	A vector consisting of zeros
$L \in \mathbb{R}^{n\times n}$	The Laplacian matrix $L = \Lambda(\mathbb{A}\mathbf{1}) - \mathbb{A}$
$\boldsymbol{u}(t) \in \mathbb{R}^n$	The inputs of the k-WTA network
$\boldsymbol{x}(t) \in \mathbb{R}^n$	The outputs of the k-WTA network
$\boldsymbol{r}_0(t), \boldsymbol{r}_i(t)$	The Cartesian coordinates of the target and the end-effector of the i-th manipulator
$\|\cdot\|_2$	The 2-norm of vectors
$\alpha, \phi, \vartheta, \rho$	Positive constants
$^{\mathrm{T}}$	The transpose symbol
Ω	$\Omega = \{\boldsymbol{x} \in \mathbb{R}^n \mid 0 \le \boldsymbol{x}_i \le 1,\ i = 1, 2, ..., n\}$
$\boldsymbol{g}(t) \in \mathbb{R}^n$	An auxiliary variable
$I_n \in \mathbb{R}^{n\times n}$	The identity matrix
$L_0 \in \mathbb{R}^{n\times n}$	$L_0 = I_n - \mathbf{1}\mathbf{1}^{\mathrm{T}}/n$
$D(t) \in \mathbb{R}^{n\times 2n}$	$D = [I_n; -I_n]$
$\boldsymbol{s}(t) \in \mathbb{R}^{2n}$	$\boldsymbol{s} = [\mathbf{1}; \mathbf{0}]$
$\boldsymbol{\sigma}(t) \in \mathbb{R}^{2n}$	An auxiliary variable
$\boldsymbol{\lambda}(t), \boldsymbol{\mu}(t)$	The Lagrange multipliers
$\circ$	The Hadamard product
$\boldsymbol{\zeta}(t) \in \mathbb{R}^n$	$\boldsymbol{\zeta}_i(t) = -\|\boldsymbol{r}_i(t) - \boldsymbol{r}_0(t)\|_2$

In this article, the manipulator whose end-effector has the smallest distance to the target is deemed the winner and assigned to execute the task. Hence, the i-th input $\boldsymbol{u}_i(t)$ is expressed as

$$\boldsymbol{u}_i(t) = -\|\boldsymbol{r}_i(t) - \boldsymbol{r}_0(t)\|_2. \tag{2}$$

Then, based on Equation (2), a QP problem is obtained as

$$\begin{aligned} &\min_{\boldsymbol{x}(t)} \frac{1}{2}\alpha\boldsymbol{x}^{\mathrm{T}}(t)\boldsymbol{x}(t) + \sum_{i=1}^{n} \boldsymbol{x}_i(t)\|\boldsymbol{r}_i(t) - \boldsymbol{r}_0(t)\|_2, \\ &\text{s.t. } \mathbf{1}^{\mathrm{T}}\boldsymbol{x}(t) = k, \\ &\quad \boldsymbol{x}(t) \in \Omega, \end{aligned} \tag{3}$$

which has been proven to be equivalent to the k-WTA operation in [9]. Subsequently, [31] describes the k-WTA operation from a new perspective in which the Laplacian matrix is introduced into the QP problem. Considering this new perspective, Equation (3) can be reformulated as

$$\begin{aligned} &\min_{\boldsymbol{x}(t)} \frac{1}{2}\alpha\boldsymbol{x}^{\mathrm{T}}(t)\boldsymbol{x}(t) + \sum_{i=1}^{n} \boldsymbol{x}_i\|\boldsymbol{r}_i(t) - \boldsymbol{r}_0(t)\|_2, \\ &\text{s.t. } \boldsymbol{x}(t) = \frac{k\mathbf{1}}{n} + L\boldsymbol{g}(t), \\ &\quad \boldsymbol{x}(t) \in \Omega, \end{aligned} \tag{4}$$

where $\mathbf{1}^{\mathrm{T}}\boldsymbol{x}(t) = k$ and $\boldsymbol{x}(t) = k\mathbf{1}/n + L\boldsymbol{g}(t)$ are equivalent if $\boldsymbol{g}(t) = L_0(L + \phi\mathbf{1}\mathbf{1}^{\mathrm{T}}/n)^{-1}\boldsymbol{x}(t) \in \mathbb{R}^n$ with $\phi > 0 \in \mathbb{R}$.

In addition, to ensure that the problem is strictly convex and has a unique stable solution, constant α has a restriction as

$$\alpha \le -\|\tilde{\boldsymbol{r}}_k(t) - \boldsymbol{r}_0(t)\|_2 + \|\tilde{\boldsymbol{r}}_{k+1}(t) - \boldsymbol{r}_0(t)\|_2, \tag{5}$$

where $\tilde{\boldsymbol{r}}_k(t)$ means the Cartesian coordinate of the k-th closest manipulator to the target and $\tilde{\boldsymbol{r}}_{k+1}(t)$ means the $(k+1)$-th one.

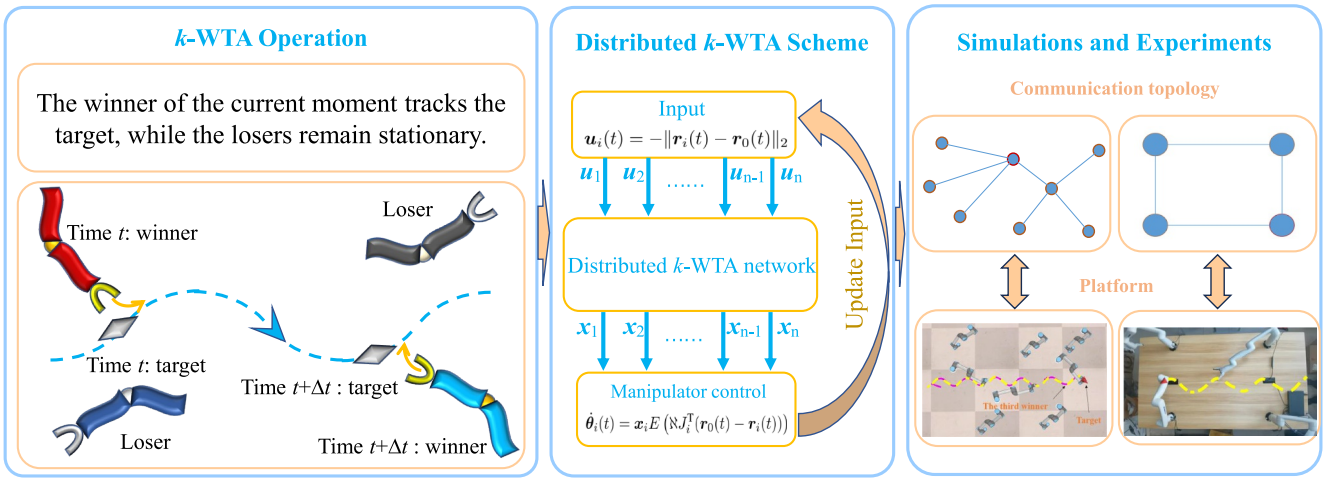


FIGURE 1 | Research framework of this article.

2.3 | Scheme Design

To solve Equation (4), the QP problem is designed with equality constraints as

$$\begin{aligned}&\min_{\boldsymbol{x}(t)} \frac{1}{2}\alpha \boldsymbol{x}^{\mathrm{T}}(t)\boldsymbol{x}(t)+\sum_{i=1}^{n}\boldsymbol{x}_i(t)\|\boldsymbol{r}_i(t)-\boldsymbol{r}_0(t)\|_2,\\ &\text{s.t. } \boldsymbol{x}(t)=\frac{k\mathbf{1}}{n}+L\boldsymbol{g}(t),\\ &\quad D(t)\boldsymbol{x}(t)+\boldsymbol{\sigma}(t)\circ\boldsymbol{\sigma}(t)=\boldsymbol{s}(t),\end{aligned} \tag{6}$$

in which $\boldsymbol{\sigma}(t)$ transforms the inequality constraint $0 \le \boldsymbol{x}_i(t) \le 1$ into an equality one. Then, the following equation can be obtained using the Lagrange multiplier method:

$$\begin{aligned}&F(\boldsymbol{x}(t),\boldsymbol{g}(t),\boldsymbol{\lambda}(t),\boldsymbol{\mu}(t),\boldsymbol{\sigma}(t))=\\ &\frac{1}{2}\alpha\boldsymbol{x}^{\mathrm{T}}(t)\boldsymbol{x}(t)+\sum_{i=1}^{n}\boldsymbol{x}_i(t)\|\boldsymbol{r}_i(t)-\boldsymbol{r}_0(t)\|_2+\boldsymbol{\lambda}^{\mathrm{T}}(t)\left(\boldsymbol{x}(t)-\frac{k\mathbf{1}}{n}-L\boldsymbol{g}(t)\right)\\ &+\boldsymbol{\mu}^{\mathrm{T}}(t)(D(t)\boldsymbol{x}(t)+\boldsymbol{\sigma}(t)\circ\boldsymbol{\sigma}(t)-\boldsymbol{s}(t)).\end{aligned} \tag{7}$$

Subsequently, the Karush–Kuhn–Tucker conditions are given by

$$\begin{cases}\alpha\boldsymbol{x}(t)-\boldsymbol{\zeta}(t)+\boldsymbol{\lambda}(t)+D^{\mathrm{T}}(t)\boldsymbol{\mu}(t)=\mathbf{0},\\ \boldsymbol{x}(t)-\dfrac{k\mathbf{1}}{n}-L\boldsymbol{g}(t)=\mathbf{0},\\ D(t)\boldsymbol{x}(t)+\Lambda(\boldsymbol{\sigma}(t))\boldsymbol{\sigma}(t)-\boldsymbol{s}(t)=\mathbf{0},\\ L\boldsymbol{\lambda}(t)=\mathbf{0},\\ 2\Lambda(\boldsymbol{\mu}(t))\boldsymbol{\sigma}(t)=\mathbf{0}.\end{cases} \tag{8}$$

For network construction, Equation (8) simplifies to $W(t)\boldsymbol{z}(t)-\boldsymbol{v}(t)=\mathbf{0}$, that is,

$$\underbrace{\begin{bmatrix}\alpha I_n & I_n & D^{\mathrm{T}}(t) & 0 & 0\\ I_n & 0 & 0 & -L & 0\\ D(t) & 0 & 0 & 0 & \Lambda(\boldsymbol{\sigma}(t))\\ 0 & L & 0 & 0 & 0\\ 0 & 0 & 0 & 0 & 2\Lambda(\boldsymbol{\mu}(t))\end{bmatrix}}_{W(t)}\underbrace{\begin{bmatrix}\boldsymbol{x}(t)\\ \boldsymbol{\lambda}(t)\\ \boldsymbol{\mu}(t)\\ \boldsymbol{g}(t)\\ \boldsymbol{\sigma}(t)\end{bmatrix}}_{\boldsymbol{z}(t)}-\underbrace{\begin{bmatrix}\boldsymbol{\zeta}(t)\\ \dfrac{k\mathbf{1}}{n}\\ \boldsymbol{s}(t)\\ \mathbf{0}\\ \mathbf{0}\end{bmatrix}}_{\boldsymbol{v}(t)}=\mathbf{0}. \tag{9}$$

To obtain the optimal solution $\boldsymbol{z}^*(t)$ of Equation (9), first, an error function is given by $\boldsymbol{\eta}(t)=W(t)\boldsymbol{z}(t)-\boldsymbol{v}(t)\in\mathbb{R}^{7n}$. Second, the NSND solver is used to make it converge to zero: $\dot{\boldsymbol{\eta}}(t)=-\vartheta P_\Omega(\boldsymbol{\eta}(t))-\rho P_\Omega\left(\boldsymbol{\eta}(t)+\vartheta\int_0^t P_\Omega(\boldsymbol{\eta}(\tau))\mathrm{d}\tau\right)$, in which $\vartheta>0$ and $\rho>0$ are used to scale the convergence rate [36], and $P_\Omega(\boldsymbol{\beta})$ is an activation function. Specifically, function $P_\Omega(\boldsymbol{\beta})$ is used in a linear form that $P_\Omega(\boldsymbol{\beta})=\boldsymbol{\beta}$. In addition, $\dot{\boldsymbol{\eta}}(t)$ can be written as $Q(t)\dot{\boldsymbol{z}}(t)-\dot{\boldsymbol{v}}(t)$ in which $Q(t)$ is expanded as follow:

$$\underbrace{\begin{bmatrix}\alpha I_n & I_n & D^{\mathrm{T}}(t) & 0 & 0\\ I_n & 0 & 0 & -L & 0\\ D(t) & 0 & 0 & 0 & 2\Lambda(\boldsymbol{\sigma}(t))\\ 0 & L & 0 & 0 & 0\\ 0 & 0 & 2\Lambda(\boldsymbol{\sigma}(t)) & 0 & 2\Lambda(\boldsymbol{\mu}(t))\end{bmatrix}}_{Q(t)}. \tag{10}$$

Finally, substituting Equations (9) and (10) and into the NSND solver and considering bounded additive noise $\boldsymbol{\iota}(t)\in\mathbb{R}^{7n}$, a D$k$-WTA network is obtained as

$$\begin{aligned}\dot{\boldsymbol{z}}(t)=\;&Q^{-1}(t)(\dot{\boldsymbol{v}}(t)-\vartheta P_\Omega(W(t)\boldsymbol{z}(t)-\boldsymbol{v}(t))-\\ &\rho P_\Omega\left(W(t)\boldsymbol{z}(t)-\boldsymbol{v}(t)+\vartheta\int_0^t P_\Omega(W(\tau)\boldsymbol{z}(\tau)-\boldsymbol{v}(\tau))\mathrm{d}\tau\right)\\ &+\boldsymbol{\iota}(t).\end{aligned} \tag{11}$$

Remark 1. In fact, perturbations such as external noises, calculation errors, and measurement errors can all be regarded as noise categories considered in this article. They can all be transformed into a part of noise $\boldsymbol{\iota}(t)$.

Remark 2. Since the traditional QP-form k-WTA problem Equation (3) involves constraint $\mathbf{1}^{\mathrm{T}}\boldsymbol{x}(t)=k$ which needs the acquisition of global information $\mathbf{1}^{\mathrm{T}}\boldsymbol{x}(t)$, most of the existing D$k$-WTA networks [18–21] are constructed by coupling a centralised k-WTA network with a consensus estimator, which complicates the model structure to some extent. To be specific, when considering the noise interference, the disturbance faced by the consensus estimator also needs to be taken into account. Moreover, when considering the lagging error problem, some existing centralised networks [29, 30] have made some achievements. However, on one hand, these networks are difficult to be distributed by directly coupling the consensus estimators due to the use of the NCP function. On the other hand, even if the consensus estimator is introduced, it is still necessary to design very large parameters for the consensus estimator to ensure the convergence of the model. In contrast, this article starts directly from solving the modified k-WTA problem Equation (6) and constructs a perturbation-resilient Dk-WTA network Equation (11) without lagging errors while avoiding problems similar to the ones mentioned above.

Remark 3. The proposed Dk-WTA network Equation (11) has more advantages in eliminating lagging errors and resisting noise interference but also brings the operation of matrix inversion, which increases the complexity of the model. It means that when the number of manipulators n is very large, the real-time performance of the system will be affected. It is worth pointing out that some existing methods such as the quasi-Newton BFGS method [37] can be considered for improving this situation.

In particular, for the i-th manipulator, Equation (8) can be reformulated as follows:

$$\begin{cases}\alpha\boldsymbol{x}_i(t)+\|\boldsymbol{r}_i(t)-\boldsymbol{r}_0(t)\|_2+\boldsymbol{\lambda}_i(t)+\boldsymbol{\mu}_i(t)-\boldsymbol{\mu}_{i+n}(t)=0,\\ \boldsymbol{x}_i(t)-\dfrac{k}{n}-\sum\limits_{j\in\mathbb{N}(i)}a_{ij}\left(\boldsymbol{g}_i(t)-\boldsymbol{g}_j(t)\right)=0,\\ \boldsymbol{x}_i(t)+\boldsymbol{\sigma}_i^2(t)-1=\boldsymbol{x}_i(t)-\boldsymbol{\sigma}_{i+n}^2(t)=0,\\ \sum\limits_{j\in\mathbb{N}(i)}a_{ij}\left(\boldsymbol{\lambda}_i(t)-\boldsymbol{\lambda}_j(t)\right)=0,\\ 2\boldsymbol{\mu}_i(t)\boldsymbol{\sigma}_i(t)=2\boldsymbol{\mu}_{i+n}(t)\boldsymbol{\sigma}_{i+n}(t)=0.\end{cases} \tag{12}$$

According to Equation (9), the above equation can be transformed into the form of $\boldsymbol{\eta}_i(t)=W_i(t)\boldsymbol{z}_i(t)-\boldsymbol{v}_i(t)\in\mathbb{R}^7$, where

$W_i(t) = \Big[\alpha, 1, 1, -1, 0, \ 0, 0; 1, 0, 0, 0, -\sum_{j\in\mathbb{N}(i)} a_{ij}, 0; 1, 0, \ 0, 0, 0, \boldsymbol{\sigma}_i(t), \ 0; -1, 0, 0, 0, 0, 0, \boldsymbol{\sigma}_{i+n}(t); 0, \sum_{j\in\mathbb{N}(i)} a_{ij}, 0, 0, 0, 0, 0; 0, 0, 0, 0, 0, 2\boldsymbol{\mu}_i(t), 0; 0, 0, 0, 0, 0, 0, 0, 2\boldsymbol{\mu}_{i+n}(t)\Big]$, $\boldsymbol{z}_i(t) = \big[\boldsymbol{x}_i(t), \boldsymbol{\lambda}_i(t), \ \boldsymbol{\mu}_i(t), \boldsymbol{\mu}_{i+n}(t), \boldsymbol{g}_i(t), \boldsymbol{\sigma}_i(t), \boldsymbol{\sigma}_{i+n}(t)\big]^{\mathrm{T}}$, and $\boldsymbol{v}_i(t) = \Big[\boldsymbol{\zeta}_i(t), \frac{k}{n} - \sum_{j\in\mathbb{N}(i)} a_{ij}\boldsymbol{g}_j(t), 1, 0, \sum_{j\in\mathbb{N}(i)} a_{ij}\boldsymbol{\lambda}_j(t), 0, 0\Big]$. Then, taking the derivative of the above equation with respect to time yields $Q_i(t)\dot{\boldsymbol{z}}_i(t) - \dot{\boldsymbol{v}}_i(t)$, where $Q_i(t) = \Big[\alpha, 1, 1, \ -1, 0, 0, 0; 1, 0, 0, 0, -\sum_{j\in\mathbb{N}(i)} a_{ij}, 0; 1, 0, 0, 0, 0, 2\boldsymbol{\sigma}_i(t), 0; -1, 0, 0, 0, 0, \ 0, 2\boldsymbol{\sigma}_{i+n}(t); \ 0, \sum_{j\in\mathbb{N}(i)} a_{ij}, 0, 0, 0, 0, 0; \ 0, 0, 2\boldsymbol{\sigma}_i(t), 0, 0, 2\boldsymbol{\mu}_i(t), 0; 0, 0, 0, 2\boldsymbol{\sigma}_{i+n}(t), 0, 0, 2\boldsymbol{\mu}_{i+n}(t)\Big]$. Subsequently, according to Equation (11), the Dk-WTA network of the i-th manipulator can be expressed as

$$\begin{aligned}\dot{\boldsymbol{z}}_i(t) \ = \ & Q_i^{-1}(t)(\dot{\boldsymbol{v}}_i(t) - \vartheta P_\Omega(W_i(t)\boldsymbol{z}_i(t) - \boldsymbol{v}_i(t)) - \\ & \rho P_\Omega\Big(W_i(t)\boldsymbol{z}_i(t) - \boldsymbol{v}_i(t) + \vartheta\int_0^t P_\Omega(W(\tau)\boldsymbol{z}_i(\tau) - \boldsymbol{v}_i(\tau))\mathrm{d}\tau\Big)\Big) \\ & + \boldsymbol{\iota}_i(t),\end{aligned}$$

where each agent only needs its own information and topological neighbours' information. Therefore, the proposed Dk-WTA network is distributed. Furthermore, it can be seen that $\boldsymbol{x}_i$ is updated via Equation (11) so that it can control the i-th manipulator in real-time whether it performs a task or not. The manipulator can only move when $\boldsymbol{x}_i(t) = 1$ and it will remain stationary if $\boldsymbol{x}_i(t) = 0$. Considering the i-th manipulator, which is a $\hat{p}$-degrees-of-freedom redundant manipulator with joint angle $\boldsymbol{\theta}_i(t) \in \mathbb{R}^{\hat{p}}$, its mapping relation between the joint angle space and Cartesian space is $\Gamma(\boldsymbol{\theta}_i(t)) = \boldsymbol{r}_i(t) \in \mathbb{R}^3$, in which $\Gamma(\cdot)$ represents the nonlinear mapping function, and $\boldsymbol{r}_i(t)$ means the Cartesian coordinate of the end-effector. Then, the forward kinematics equation of manipulators can be deduced as follows:

$$J(\boldsymbol{\theta}_i(t))\dot{\boldsymbol{\theta}}_i(t) = \dot{\boldsymbol{r}}_i(t),$$

where $J(\boldsymbol{\theta}_i(t)) = \partial\Gamma(\boldsymbol{\theta}_i(t))/\partial\boldsymbol{\theta}_i(t) \in \mathbb{R}^{3\times\hat{p}}$ is the Jacobian matrix, and $\dot{\boldsymbol{\theta}}_i(t)$ is the joint angular velocity. Subsequently, for the i-th manipulator, the following equation holds:

$$\dot{\boldsymbol{\theta}}_i(t) = \frac{1}{2}\aleph\frac{\partial\boldsymbol{u}_i(t)}{\partial\boldsymbol{\theta}_i(t)} = \aleph J_i^{\mathrm{T}}(\boldsymbol{r}_0(t) - \boldsymbol{r}_i(t)), \tag{13}$$

where $\boldsymbol{u}_i(t) = -\|\boldsymbol{r}_i(t) - \boldsymbol{r}_0(t)\|_2$ with $\boldsymbol{r}_0(t)$ representing the Cartesian coordinates of the target, $\aleph$ represents the feedback gain of the joint angular velocity change, and J_i is shorthand for $J(\boldsymbol{\theta}_i(t))$. Furthermore, combined with the proposed Dk-WTA network Equation (11), the dynamic task allocation scheme can be obtained from two steps:

1. The proposed Dk-WTA network selects the winner (the manipulator closest to the target) based on the input $\boldsymbol{u}_i(t) = -\|\boldsymbol{r}_i(t) - \boldsymbol{r}_0(t)\|_2$ of each manipulator, which is the negative of the distance from the end-effector of that manipulator to the target. Specifically, the output $\boldsymbol{x}_i(t)$ corresponding to the winner is set to 1, whereas the remains are set to 0, with $\boldsymbol{x}(t) = \boldsymbol{z}(t)[1:n]$.
2. In this scheme, the winner is expected to track the target, whereas the losers need to remain on standby. Hence, according to Equation (13) and considering the limit of joint angular velocity in realistic scenes, the following equation holds:

$$\dot{\boldsymbol{\theta}}_i(t) = \boldsymbol{x}_i(t)E_i\big(\aleph J_i^{\mathrm{T}}(\boldsymbol{r}_0(t) - \boldsymbol{r}_i(t))\big),$$

in which $E_i(c)$ can be described as

$$E_i(c) = \begin{cases}\varrho_i^-, & c < \varrho_i^-, \\ c, & \varrho_i^- \le c \le \varrho_i^+, \\ \varrho_i^+, & c > \varrho_i^+.\end{cases}$$

Evidently, as the winner and target move, the input $\boldsymbol{u}_i(t) = -\|\boldsymbol{r}_i(t) - \boldsymbol{r}_0(t)\|_2$ of each manipulator changes accordingly. This may cause the winner of the first step to change, which in turn has an impact on the second step. Thus, as shown in the middle part of Figure 1, the overall scheme can be viewed as a loop between the two steps. In a word, the scheme can be summarised as follows:

$$\begin{cases}\dot{\boldsymbol{z}}(t) = Q^{-1}(t)(\dot{\boldsymbol{v}}(t) - \vartheta P_\Omega(W(t)\boldsymbol{z}(t) - \boldsymbol{v}(t)) - \\ \rho P_\Omega\Big(W(t)\boldsymbol{z}(t) - \boldsymbol{v}(t) + \vartheta\int_0^t P_\Omega(W(\tau)\boldsymbol{z}(\tau) \\ \quad - \boldsymbol{v}(\tau))\mathrm{d}\tau\Big) + \boldsymbol{\iota}(t), \\ \dot{\boldsymbol{\theta}}_i(t) = \boldsymbol{x}_i(t)E_i\big(\aleph J_i^{\mathrm{T}}(\boldsymbol{e}_0(t) - \boldsymbol{e}_i(t))\big), \\ \boldsymbol{x}(t) = \boldsymbol{z}(t)[1:n].\end{cases} \tag{14}$$

3 | Theoretical Analyses

Three theorems are provided and proved in this section. Two of them analyse the convergence of the NSND solver for each manipulator used in the proposed Dk-WTA scheme Equation (14) without and with noise. In the last one, the equivalence of Equations (3) and (4) is proved.

Theorem 1. *Without considering noises, the i-th manipulator decides independently whether to perform the task or not based on its own information and information of the topological neighbours. That is, during the k-WTA problem-solving process, the variable* $\boldsymbol{z}_i(t) = \big[\boldsymbol{x}_i(t), \boldsymbol{\lambda}_i(t), \boldsymbol{\mu}_i(t), \boldsymbol{\mu}_{i+n}(t), \boldsymbol{g}_i(t), \boldsymbol{\sigma}_i(t), \boldsymbol{\sigma}_{i+n}(t)\big]^{\mathrm{T}}$ *converges globally to the theoretical solution* $\boldsymbol{z}_i^*(t)$ *in which* $\boldsymbol{x}_i^*(t)$ *is the drive command signal for the i-th manipulator. Proof: First of all, for the convenience of proving, an auxiliary equation is given as:*

$$\boldsymbol{\chi}_i(t) = \boldsymbol{\eta}_i(t) + \vartheta\int_0^t P_\Omega\big(\boldsymbol{\eta}_i(\tau)\big)\mathrm{d}\tau \in \mathbb{R}^{7n}. \tag{15}$$

The time derivative of this equation can be written as follows:

$$\dot{\boldsymbol{\chi}}_i(t) = \dot{\boldsymbol{\eta}}_i(t) + \vartheta P_\Omega\big(\boldsymbol{\eta}_i(t)\big). \tag{16}$$

Combining the NSND solver with Equation (16), an equation is obtained as

$$\dot{\boldsymbol{\chi}}_i(t) = -\rho P_\Omega\big(\boldsymbol{\chi}_i(t)\big). \tag{17}$$

Then, a Lyapunov candidate function is designed as

$$\mathcal{L}_1(t) = \frac{1}{2}\chi_i^{\mathrm{T}}(t)\chi_i(t). \tag{18}$$

It can be concluded from Equation (18) that only when $\chi_i(t) = \mathbf{0}$, $\mathcal{L}_1(t) = 0$; otherwise, $\mathcal{L}_1(t) > 0$. Furthermore, taking Equation (17) into account, the time derivative of Equation (18) is obtained as

$$\dot{\mathcal{L}}_1(t) = -\rho\chi_i^{\mathrm{T}}(t)P_\Omega(\chi_i(t)). \tag{19}$$

Referring to the activation function $P_\Omega(\cdot)$ used in this article, it is easy to obtain

$$\|P_\Omega(\chi_i(t)) - \chi_i(t)\|_2^2 \le \|\xi - \chi_i(t)\|_2^2, \quad \xi \in \Omega.$$

If $\xi = \mathbf{0}$, according to the properties of 2-norm, one can obtain

$$2P_\Omega^{\mathrm{T}}(\chi_i(t))\chi_i(t) \ge P_\Omega^{\mathrm{T}}(\chi_i(t))P_\Omega(\chi_i(t)) > 0,$$

from which the following inequality can be concluded as

$$0 < \frac{1}{2}\rho P_\Omega^{\mathrm{T}}(\chi_i(t))P_\Omega(\chi_i(t)) \le -\dot{\mathcal{L}}_1(t).$$

From the preceding derivation, it is evident that $\chi_i(t)$ approaches zero in a global manner. Applying LaSalle's invariance principle and Equation (16) yields the subsequent expression:

$$\dot{\eta}_i(t) = -\vartheta P_\Omega(\eta_i(t)). \tag{20}$$

Another Lyapunov candidate function is given by

$$\mathcal{L}_2(t) = \frac{1}{2}\eta_i^{\mathrm{T}}(t)\eta_i(t). \tag{21}$$

It can be seen that Equations (20) and (21) are similar to Equations (17) and (18) so that the theorem that $\eta_i(t)$ is globally convergent to zero can be proved by the same method. Since $\eta_i(t) = W_i(t)z_i(t) - v_i(t)$, $z_i(t) = \left[x_i(t), \lambda_i(t), \mu_i(t), \mu_{i+n}(t), g_i(t), \sigma_i(t), \sigma_{i+n}(t)\right]^{\mathrm{T}}$ approaches the theoretical solution $z_i^*(t)$ in which $x_i^*(t)$ is used to control the i-th manipulator. The proof is thus completed. ■

In this article, the linear activation function is used and an arbitrary bounded disturbance is added to the Equation (11). Accordingly, the noise of the i-th manipulator is expressed as $\iota_i(t)$. Considering the above factors, the following theorem needs to be proved.

Theorem 2. *If ϑ and ρ are large enough, under the condition of an arbitrary bounded noise $\iota_i(t)$, the i-th manipulator decides independently whether to perform the task or not based on its own information and information of the topological neighbours. That is, $x_i(t)$ approaches the theoretical solution $x_i^*(t)$.*

Proof: Considering the linear activation function and the error vector $\eta_i(t)$, it can be obtained that

$$\dot{\eta}_i(t) = -(\vartheta + \rho)\eta_i(t) - \vartheta\rho\int_0^t \eta_i(\tau)\mathrm{d}\tau + \iota_i(t).$$

Then, using the Laplace transform, the result obtained can be reformulated as

$$M_i(s) = O(s)H_i(s), \tag{22}$$

where $M_i(s)$ and $H_i(s)$ are the Laplace transform of $\eta_i(t)$ and $\iota_i(t)$. Laplace transform $O(s)$ is given by

$$O(s) = \frac{s}{s^2 + (\vartheta + \rho)s + \vartheta\rho}.$$

Letting $s = j\omega$, $|O(j\omega)|^2$ can be written as

$$|O(j\omega)|^2 = \frac{\omega^2}{\omega^4 + (\vartheta^2 + \rho^2)\omega^2 + \vartheta^2\rho^2} = \frac{1}{\omega^2 + \frac{\vartheta^2\rho^2}{\omega^2} + (\vartheta^2 + \rho^2)}.$$

Based on the property of mean value inequality, one can obtain that if $\omega^2 = \vartheta\rho$, $|O(j\omega)|^2$ can be maximised. In addition, the maximum of $|O(j\omega)|$ is $1/(\vartheta + \rho)$. It can be concluded from the result that increasing ϑ and ρ leads to a smaller $|O(t)|$. Then, according to Equation (22), the relationship between $\eta_i(t)$ and $\iota_i(t)$ can be acquired as

$$\eta_{ip}(t) = \int_0^t \iota_{ip}(t-\tau)O(\tau)\mathrm{d}\tau,$$

in which $1 \le p \le 7$. Because $\iota_i(t)$ is bounded, let m be the upper bound of the noise, and one can obtain that

$$\max_{1\le p\le 7}|\eta_{ip}(t)| = \max_p\left|\int_0^t \iota_{ip}(t-\tau)O(\tau)\mathrm{d}\tau\right| \le m\int_0^t |O(\tau)|\mathrm{d}\tau.$$

Therefore, $O(t)$ imposes a restriction on $\iota_i(t)$. If ϑ and ρ become larger, $|O(t)|$ will be smaller so that $|\eta_i(t)|$ has smaller variation range. Similarly, the theorem that during the k-WTA problem-solving process, $x_i(t)$ approaches the theoretical solution $x_i^*(t)$ can be proved by the same process as in Theorem 1. The proof is thus completed. ■

Although larger values of ϑ and ρ imply a faster convergence rate and smaller residual errors, they also require higher requirements for both the software and hardware. Therefore, the values of parameters cannot be unlimitedly large.In Section 2.2, the condition of equivalence between the two constraints is briefly mentioned. The relevant proof is given below.

Theorem 3. *When $g(t) = L_0(L + \phi\mathbf{1}\mathbf{1}^{\mathrm{T}}/n)^{-1}x(t) \in \mathbb{R}^n$ with $\phi > 0 \in \mathbb{R}$, the conventional equality constraint $\mathbf{1}^{\mathrm{T}}x(t) = k$ in Equation (3) is equivalent to $x(t) = k\mathbf{1}/n + Lg(t)$ in Equation (4).*

Proof: Considering $\mathbf{1}^{\mathrm{T}}x(t) = k$ and $L_0 = I_n - \mathbf{1}\mathbf{1}^{\mathrm{T}}/n$, this yield the following equation:

$$x(t) = \frac{k\mathbf{1}}{n} + L_0x(t).$$

According to the property of Laplacian matrix: $L\mathbf{1} = \mathbf{0}$, one can obtain that

$$LL_0 = L = L_0L. \tag{23}$$

Referring to [31], $L + \phi\mathbf{1}\mathbf{1}^{\mathrm{T}}/n$ is invertible. Then, combined with Equation (23) and the above property, the following formula can be gotten as

$$\begin{aligned}\boldsymbol{x}(t) &= \frac{k\mathbf{1}}{n} + L_0\left(L + \phi\frac{\mathbf{1}\mathbf{1}^{\mathrm{T}}}{n}\right)\left(L + \phi\frac{\mathbf{1}\mathbf{1}^{\mathrm{T}}}{n}\right)^{-1}\boldsymbol{x}(t)\\ &= \frac{k\mathbf{1}}{n} + L_0 L\left(L + \phi\frac{\mathbf{1}\mathbf{1}^{\mathrm{T}}}{n}\right)^{-1}\boldsymbol{x}(t)\\ &= \frac{k\mathbf{1}}{n} + LL_0\left(L + \phi\frac{\mathbf{1}\mathbf{1}^{\mathrm{T}}}{n}\right)^{-1}\boldsymbol{x}(t)\\ &= \frac{k\mathbf{1}}{n} + L\boldsymbol{g}(t),\end{aligned}$$

in which $\boldsymbol{g}(t) = L_0\left(L + \phi\mathbf{1}\mathbf{1}^{\mathrm{T}}/n\right)^{-1}\boldsymbol{x}(t)$. Moreover, the necessity of this theorem needs to be proved. Considering $\mathbf{1}^{\mathrm{T}}L = \mathbf{0}$, the following derivation is given as

$$\mathbf{1}^{\mathrm{T}}\boldsymbol{x}(t) = \frac{\mathbf{1}^{\mathrm{T}}\mathbf{1}k}{n} + \mathbf{1}^{\mathrm{T}}L\boldsymbol{g}(t) = \frac{\mathbf{1}^{\mathrm{T}}\mathbf{1}k}{n} = k.$$

So far, the equivalence of the constraints is proved. ■

Moreover, note that the proof of Theorem 3 requires the use of the property: $L1 = 1^{\mathrm{T}}L = 0$, whose derivation utilises the symmetry of the adjacency matrix $\mathbb{A}$. That is, it requires that the corresponding topological structure is undirected.

4 | Simulations and Results Analyses

In this section, comparisons between the proposed Dk-WTA scheme Equation (14) and other ones are conducted. Then, using scheme Equation (14) proposed in this article, simulations and experiments are demonstrated, which are conducted on eight UR5 manipulators and a multi-manipulator platform with four KINOVA Gen3 lite manipulators, respectively.

4.1 | Comparisons With Existing Studies

In Table 2, distributed k-WTA schemes in different articles are compared with each other. On the one hand, from the perspective of network structure [18–21], all suffer from lagging errors and do not consider noise interference. Besides, these distributed k-WTA networks are constructed by introducing a consensus estimator. It means that the convergence performance and disturbance resistance of the consensus estimator should also be taken into account, which will further complicate the problems. Although [31] present a new idea and construct a distributed network without introducing a consensus estimator, as shown in the simulations above, the lagging error problem and noise problem remain unsolved. On the other hand, from the perspective of applications [19, 20, 31], all treat each agent in the k-WTA network as a particle, which indicates that the nonlinearity of an agent is not considered, and thus it is difficult to apply to specific application scenarios. Generally speaking, the proposed distributed k-WTA network Equation (11) which is further combined with forward kinematics to obtain a distributed dynamic task allocation scheme for multiple manipulators Equation (14) has no lagging errors, considers noise interference, and does not need to introduce a consensus estimator.

To more intuitively illustrate the advantages of the proposed Dk-WTA network in terms of lagging errors and noise issues. We select the k-WTA networks from [21, 31] for comparison based on the numerical simulation. The first one [31] is shown as follows:

$$\begin{aligned}\dot{\boldsymbol{x}}(t) &= \frac{1}{\varpi\alpha}\left(-\alpha\boldsymbol{x}(t) + \alpha\mathcal{G}\left(\boldsymbol{u}(t) - \frac{\boldsymbol{\kappa}(t)}{\alpha}\right)\right),\\ \dot{l}(t) &= \frac{1}{\varpi\alpha}L\boldsymbol{\kappa}(t),\\ \dot{\boldsymbol{\kappa}}(t) &= \frac{1}{\varpi\alpha}\left(\boldsymbol{x}(t) - \frac{k\mathbf{1}}{n} - Ll(t) - L\boldsymbol{\kappa}(t)\right),\end{aligned} \tag{24}$$

where $1/(\varpi\alpha)$ is the convergence coefficient with $\varpi > 0$ and $l(t)$ and $\boldsymbol{\kappa}(t)$ are state variables. For $\mathcal{G}_i(\mathfrak{g})$, if $0 < \mathfrak{g} < 1$, $\mathcal{G}_i(\mathfrak{g}) = \mathfrak{g}$, while if $\mathfrak{g} \le 0$ or $\mathfrak{g} \ge 1$, $\mathcal{G}_i(\mathfrak{g})$ will remain 0 or 1, respectively. Furthermore, the formulation of the second one [21] can be obtained as follows:

$$\begin{aligned}\dot{p}(t) &= -\mathfrak{c}\left(q(t) + \boldsymbol{x}(t) + Lp(t) - \frac{k\mathbf{1}}{n}\right),\\ \dot{q}(t) &= -\mathfrak{c}(Lp(t) + Lq(t)),\\ \boldsymbol{x}(t) &= \mathcal{G}\left(p(t) + \frac{\boldsymbol{u}(t)}{\alpha}\right),\end{aligned} \tag{25}$$

TABLE 2 | Comparisons of Dk-WTA schemes.

	QP problem	Noise considered	Consensus estimators	Input type*	Application scenarios	Experimental verification
Scheme (14)	L_+	Yes	No	Time-varying inputs	Multiple manipulators	Yes
Scheme in [18]	L_-	No	Yes	Constant inputs	Multiple manipulators	No
Scheme in [19]	L_-	No	Yes	Constant inputs	Multiple agent#	No
Scheme in [20]	L_-	No	Yes	Constant inputs	Multiple agent#	No
Scheme in [21]	L_-	No	Yes	Constant inputs	Multiple manipulators	No
Scheme in [31]	L_+	No	No	Constant inputs	Multiple agent#	No

Note: L_+: The QP-form k-WTA problem introduces the Laplacian matrix. L_-: The QP-form k-WTA problem does not introduce the Laplacian matrix. *: Some schemes are not suitable for handling time-varying inputs due to large lagging errors. #: Each agent is considered as a point mass, which means that the nonlinearity of an agent is not considered.

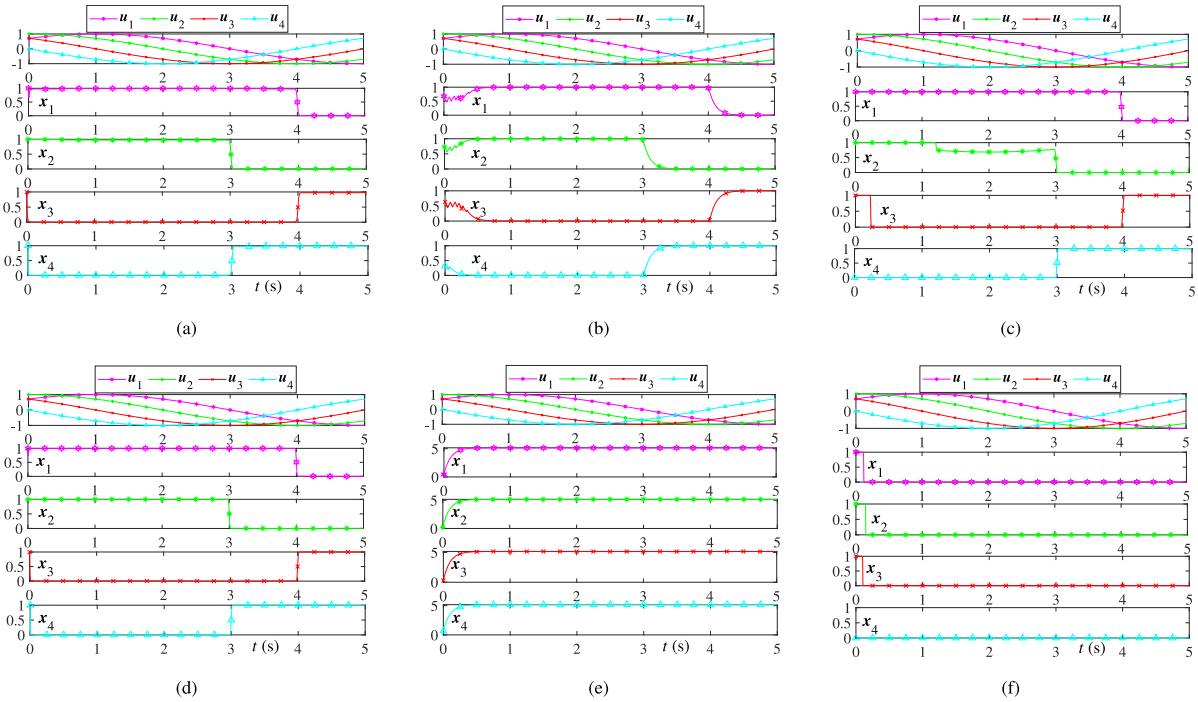


FIGURE 2 | Comparisons among the proposed Dk-WTA network Equation (11), network Equation (24), and network Equation (25), where four sine functions are used to model the input $\boldsymbol{u}(t)$. (a) $\boldsymbol{x}(t)$ produced by the proposed Dk-WTA network Equation (11) when no noise is present. (b) $\boldsymbol{x}(t)$ produced by network Equation (24) when no noise is present. (c) The outputs $\boldsymbol{x}(t)$ of network Equation (25) when no noise is present. (d) $\boldsymbol{x}(t)$ produced by the proposed Dk-WTA network Equation (11) when noise is present. (e) $\boldsymbol{x}(t)$ produced by network Equation (24) when noise is present. (f) $\boldsymbol{x}(t)$ produced by network Equation (25) when noise is present.

where $p(t)$ and $q(t)$ are state variables and $\mathfrak{c}$ is a positive constant.

Then, for comparison purposes, we use four sine functions ($n = 4$) to model the inputs to the k-WTA network, ensuring two winners will emerge ($k = 2$). Specifically, for $i = 1, 2, 3, 4$, let $\boldsymbol{u}_i(t) = \sin(0.25\pi(t + i))$. The communication topology is shown in Figure 1. For the proposed Dk-WTA network Equation (11), it has $\alpha = 0.01$, $\vartheta = 1000$, and $\rho = 5 \times 10^{-3}$, while for network Equation (24) and network Equation (25), they have the same convergence coefficient, that is, $1/(\varpi\alpha) = \mathfrak{c} = \vartheta = 1000$. As observed in Figure 2a–b, when no noise is present, the proposed Dk-WTA network Equation (11) exhibits a faster response when winners change due to the absence of lagging errors. In contrast, network Equation (24) and network Equation (25) exhibit varying degrees of hysteresis and instability. Furthermore, we add noise $50 \times \mathbf{1} + \boldsymbol{\epsilon}(t)$ with each element in $\boldsymbol{\epsilon}(t)$ taking a random value from 0 to 3 to both networks, and parameter ρ is reset to 5×10^{-2} in the proposed Dk-WTA network Equation (11). Evidently, in Figure 2d, the proposed Dk-WTA network Equation (11) still works well, whereas in Figure 2e,f, network Equation (24) and network Equation (25) have collapsed. Besides, to make a more intuitive comparison among the proposed Dk-WTA network Equation (11), network Equation (24), and network Equation (25), we introduce a new metric. According to Equation (3), $\boldsymbol{x}(t)$ produced by a k-WTA network should satisfy $|\mathbf{1}^{\mathrm{T}}\boldsymbol{x}(t) - k| = 0$. Hence, we compare the values of $|\mathbf{1}^{\mathrm{T}}\boldsymbol{x}(t) - k|$ in Figure 3 for the three networks with and without noises, respectively. As shown in the top half of Figure 3, in the absence of noises, only the proposed Dk-WTA network Equation (11) satisfies $|\mathbf{1}^{\mathrm{T}}\boldsymbol{x}(t) - k| = 0$ quickly at the beginning of the simulation, whereas the other two networks have different degrees of lag. Meanwhile, in the noisy case, as shown in the

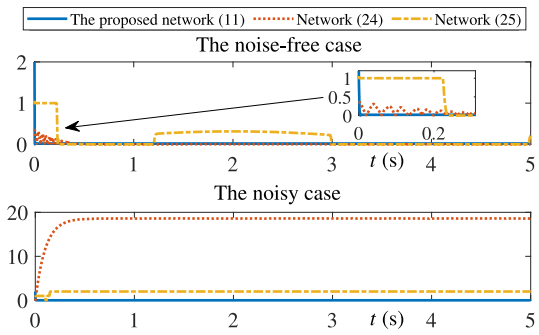


FIGURE 3 | Changes in $|\mathbf{1}^{\mathrm{T}}\boldsymbol{x}(t) - k|$ of the proposed Dk-WTA network Equation (11), network Equation (24), and network Equation (25) on the numerical simulations with inputs $\boldsymbol{u}_i(t) = \sin(0.25\pi(t + i))(i \in \{1, 2, 3, 4\})$.

TABLE 3 | Comparisons among different Dk-WTA networks on convergence time.

k-WTA networks	Noise-free condition	Noisy condition
The proposed Dk-WTA network Equation (11)	< 0.010 s	< 0.010 s
Network in [31] Equation (24)	0.374 s	NA
Network in [21] Equation (25)	0.234 s	NA

Note: NA represents that the k-WTA network collapses and fails to converge.

bottom half of Figure 3, $|\mathbf{1}^{\mathrm{T}}\boldsymbol{x}(t) - k| = 0$ cannot be satisfied by network Equation (24) and network Equation (25), whereas the proposed Dk-WTA network Equation (11) still operates normally. Besides, the more specific comparative results are presented in Table 3. Overall, the advantages of the proposed Dk-WTA network Equation (11) on the lagging error problem and the noise problem are verified.

Remark 4. From the perspective of the model, $\vartheta + \rho$ acts as the coefficient of the scale term, and the larger its value, the faster the convergence rate of the model. Furthermore, the integral term has the ability to suppress bounded noises. With the increase of parameter $\vartheta\rho$, the inhibition ability will be stronger. However, if the parameter of the integral term is too large, the convergence accuracy of the model will be affected to a certain extent. To further illustrate the influence of parameter selection on the proposed Dk-WTA network Equation (11), based on the above numerical simulation settings, as shown in Figure 4, we provide parameter sensitivity analyses under noisy and noise-free conditions, respectively, where the number in each grid represents the actual value of $|\mathbf{1}^{\mathrm{T}}\boldsymbol{x}(t) - k|$ (the theoretical value is 0) in the steady state. It is worth pointing out that although $|\mathbf{1}^{\mathrm{T}}\boldsymbol{x}(t) - k|$ sometimes fails to accurately converge to the theoretical value 0 due to the size of the integral term parameter or the existence of noises in the simulations, the proposed Dk-WTA network Equation (11) can still quickly and correctly distinguish the winners and losers, rather than the direct collapse as in other networks (Equations 24 and 25), which further illustrates the robustness of the proposed Dk-WTA network Equation (11).

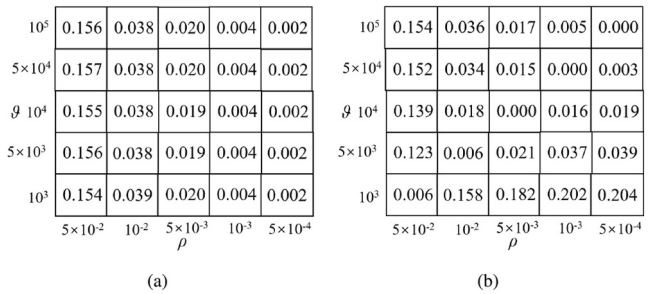


FIGURE 4 | Parameter sensitivity analyses of the model under noisy and noise-free conditions with each grid representing the actual value of $|\mathbf{1}^{\mathrm{T}}\boldsymbol{x}(t) - k|$ (the theoretical value is 0) in the steady state. (a) Noise-free condition. (b) Noisy condition.

4.2 | Simulations and Experiments

Specifically, parameters used in the simulation are defined as follows: the count of manipulators $n = 8$; the count of winners performing the tracking task $k = 1$; the location of the eight manipulators $[0, 0, 0; 0.4, 1, 0; 1, -0.73, 0; 2, 0.8, 0; 2.4, 0.2, 0; 1, -1, 0; 2.4, -0.9, 0; 3, 0.9, 0]$ m; the initial joint angles of the manipulators $[\pi/4, -\pi/4, \pi/2, \pi/4, \pi/2, 0; \pi/4, -\pi/4, \pi/2, \pi/4, \pi/2, 0; 3\pi/2, -\pi/4, \pi/2, \pi/4, \pi/2, 0; \pi/4, -\pi/4, \pi/2, \pi/4, \pi/2, 0; \pi/4, -\pi/4, \pi/2, \pi/4, \pi/2, 0; \pi/4, -\pi/4, \pi/2, \pi/4, \pi/2, 0; \pi/4, -\pi/4, \pi/2, \pi/4, \pi/2, 0]$ rad; the initial position of the target $[-0.6; -0.4; 0.0303]$ m; the velocity of the target $[0.1, 0.1\sin(t), 0]$ m/s; the feedback gain of the joint angular velocity change $\aleph = 30$; $\alpha = 0.01$; $\vartheta = 10000$; $\rho = 10^{-3}$; $\varrho_i^{+} = |\varrho_i^{-}| = 0.6$ rad/s; noise $\iota(t)$ is set to $7 \times \mathbf{1} + \boldsymbol{\epsilon}(t)$ with each element in $\boldsymbol{\epsilon}(t)$ taking a random value from 0 to 1; the communication topology used for the simulations

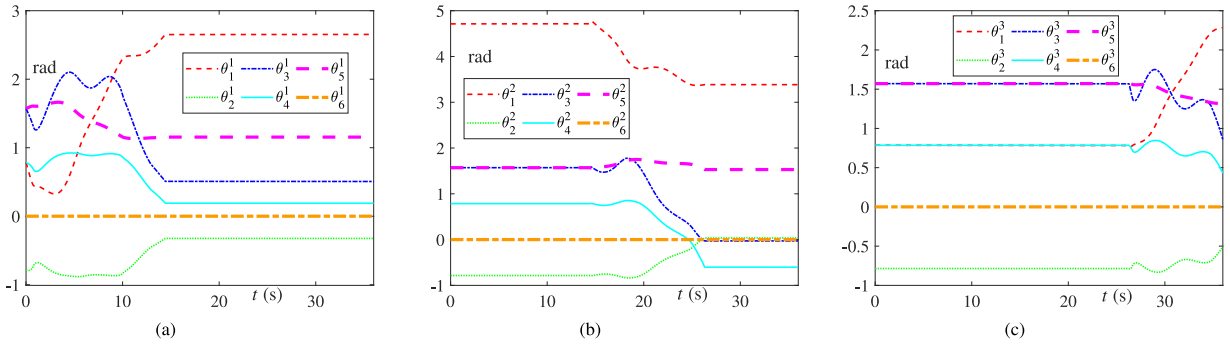


FIGURE 5 | Joint-angle curves of the three winners. (a) First. (b) Second. (c) Third.

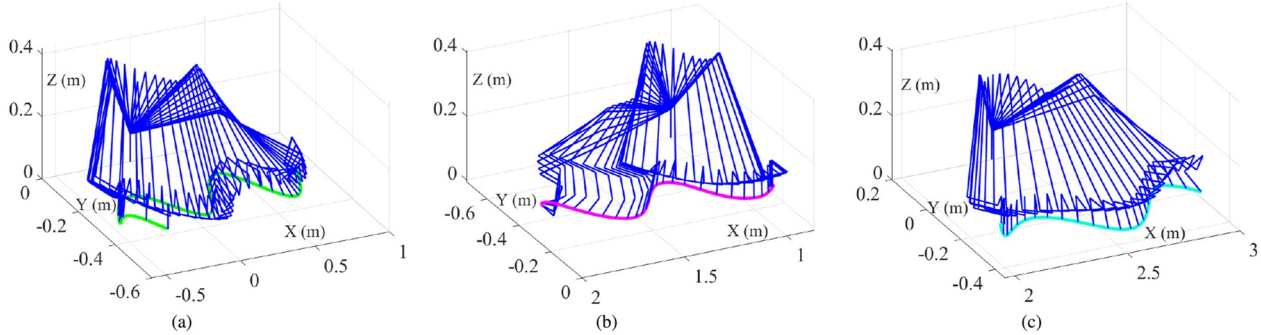


FIGURE 6 | Dynamic changes of three winners during the tracking process. (a) First. (b) Second. (c) Third.

is shown in Figure 1. As the simulation begins, the target moves from its initial position. At this point, each manipulator makes a judgement about whether its end-effector has the smallest distance to the target based on the information about itself and the topological neighbours. The corresponding drive command signal $\boldsymbol{x}_i$ converges quickly according to the judgement result. Then, the first winner emerges to perform the task of tracking the target, whereas the rest of the manipulators remain motionless as losers. The change in the joint angles and the dynamic tracking process of the manipulator as the first winner are respectively shown in Figures 5a, 6a. As shown in Figure 7b, in tandem with the target's motion, the first winner is no longer the best choice for real-time target tracking due to the limitations of the physical size of the manipulator. Hence, each manipulator reasserts its judgement on whether it is performing the task or not and the drive command signal $\boldsymbol{x}_i(t)$ converges to a new value so that the second winner emerges. That is, from a global perspective, the k-WTA network selects the best choice for the task at the current moment from all manipulators. Figure 7a shows that the change time of the drive command signal is less than 0.07 s when the change of winner occurs. Similarly, the second winner alternates with the third winner in the same process as above. Finally, Figure 7b presents the simulation results. In the meantime, for visualising the manipulator's motion state throughout the tracking process, the corresponding simulation is performed on the CoppeliaSim platform which uses the same initial position information and the same parameters. By observing the simulation results shown in Figure 8, one finds that the manipulators smoothly complete the task of target trajectory tracking.

Furthermore, for verification of the scalability of the proposed scheme Equation (14), further experiments are presented on a multi-manipulator platform with four KINOVA Gen3 lite manipulators. Specifically, the size of the platform is 1.2 × 2.2 m; the longitudinal and lateral distances of each manipulator from the edges of the platform are 0.15 and 0.48 m, respectively; the communication topology used for the experiments is shown in Figure 1; the settings of the parameters in the proposed scheme Equation (14) are the same as those in the simulations. Furthermore, for illustration purposes, as shown in the first picture in Figure 9, we first label each manipulator and establish the coordinate system with the centre of the base of Manipulator 1 as the origin, where the height of the desktop is treated as 0 m. Then, the base centre coordinates of these four manipulators are [0, 0, 0] m, [0, 0.9, 0] m, [1.24, 0.9, 0] m, and [1.24, 0, 0] m, respectively. Their initial joint angles are [2.14, −0.9, 1.05, 1.5, 0.89, −0.79] rad, [3.14, −0.79, 1.37, 1.57, 0.79, −0.79] rad, [−0.59, −1.18, 0.59, 1.57, 0.79, −0.79], and [0, −0.79, 1.37, 1.57, 0.79, −0.79] rad, respectively. In addition, the tracked target has an initial position of [−0.48, 0.41, 0.11] m, as well as a velocity of [0.1, 0.1*sin(t), 0] m/s. Besides, $\boldsymbol{x}_i(t)$ produced by the proposed Dk-WTA network Equation (11) corresponding to each manipulator over time during task execution is shown in Figure 10. Note that the proposed Dk-WTA network successfully selects the winner and converges quickly when the winner switches. Correspondingly, as shown in Figure 9, the two winners alternately perform and complete the trajectory tracking task in the experiment.

Overall, a centralised k-WTA network requires a unified scheduling module for task assignment when performing the same task, whereas the distributed task dynamic assignment process is performed spontaneously by each agent through information about itself and the neighbours within the topological

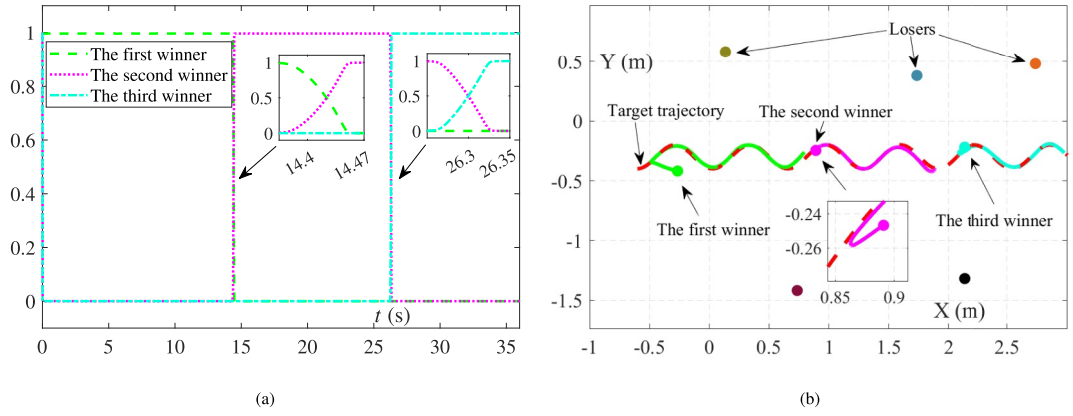


FIGURE 7 | Simulation of eight UR5 manipulators with task duration 36 s. (a) Update of the drive command signal $\boldsymbol{x}_i$ of three winners. (b) Process of three winners performing the trajectory-tracking task alternately.

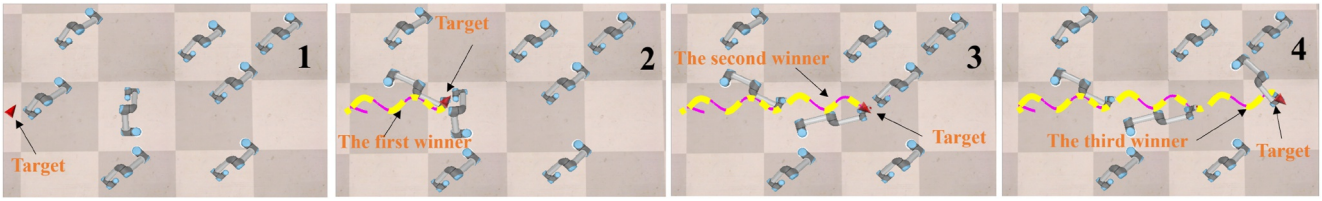


FIGURE 8 | Snapshots of the simulation based on eight UR5 manipulators on the CoppeliaSim platform, where three winners alternately perform a trajectory-tracking task, whereas other manipulators stay still. The simulation video is available at https://youtu.be/gWyzeO-z5qI and https://www.bilibili.com/video/BV1URA3e1Ef7.

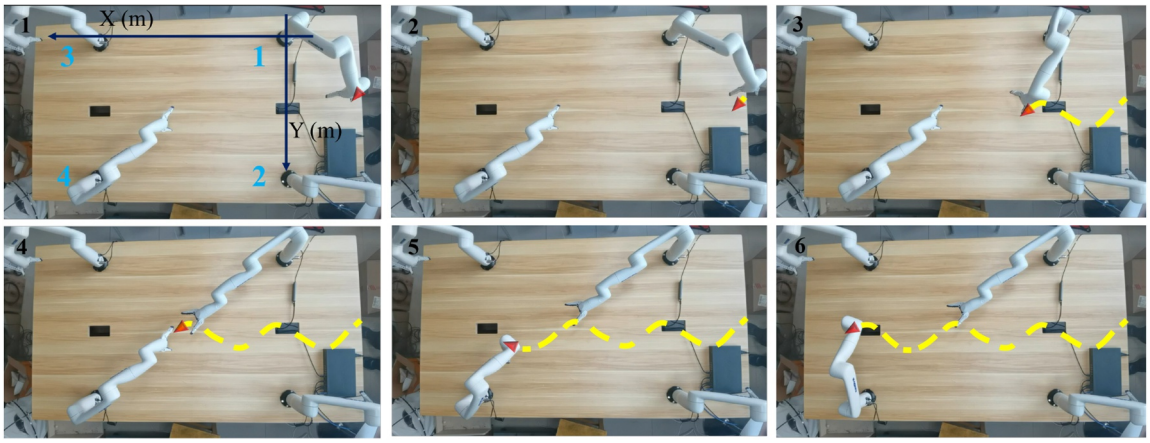


FIGURE 9 | Snapshots of the experiment based on a multi-manipulator platform with four KINOVA Gen3 lite manipulators, where two winners alternately perform a trajectory-tracking task, whereas other manipulators stay still. The experimental video is available at https://youtu.be/eGKm6nCO_i8 and https://www.bilibili.com/video/BV1moA3e5Eyd.

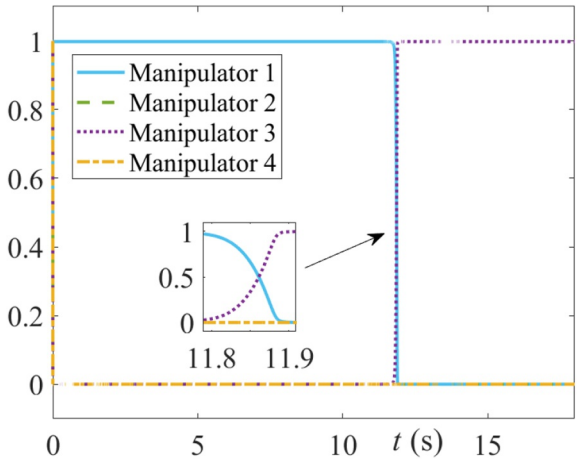


FIGURE 10 | Changes of $\boldsymbol{x}(t)$ produced by the proposed Dk-WTA network Equation (11) in the multiple KiNOVA Gen3 lite manipulator experiment.

domain. Moreover, the criteria used to determine winners are not unique and related to the properties of each agent and specific application scenarios. For example, the residual energy of each manipulator can be considered as part of the input information, in which the input to the i-th manipulator $\boldsymbol{u}_i(t)$ can be written as follows:

$$\boldsymbol{u}_i(t) = -\|\boldsymbol{r}_i(t) - \boldsymbol{r}_0(t)\|^2 + \mathfrak{d}e_i(t),$$

where $\mathfrak{d} \in \mathbb{R}^+$ is a weight coefficient; $e_i(t)$ represents the residual energy of the i-th manipulator. That is, manipulators with higher residual energy and closer to the target are given priority to perform tasks. Then, the above equation can be generalised to a more general form:

$$\boldsymbol{u}_i(t) = -\|\boldsymbol{r}_i(t) - \boldsymbol{r}_0(t)\|^2 + \sum_{j=1} \mathfrak{d}_j e_{ij}(t),$$

where $e_{ij}(t)$ represents the j-th attribute of the i-th manipulator with $\mathfrak{d}_j$ being the corresponding weight. Hence, this competition-based coordination ensures optimal agent selection, such that the entire system can fulfil tasks with minimum resource expenditure.

Remark 5. The core of the proposed Dk-WTA scheme is to decide whether each manipulator performs the task or not based on the output $\boldsymbol{x}(t)$ of the proposed Dk-WTA network. Hence, in the above simulations and experiments, with the movement of the target, the output of the k-WTA network controlling the manipulators can change rapidly to realize the switch of the winner manipulator performing the task and ensure the continuous tracking of the target, which means the success of the trajectory-tracking task.

5 | Conclusions

In this article, a new Dk-WTA network considering both lagging errors and noise interference has been proposed, which does not require the introduction of a consensus estimator. Then, combined with the forward kinematics, a new Dk-WTA dynamic allocation scheme used for competitive coordination of multiple manipulators has been constructed. In this scheme, each manipulator makes a judgement based on its own and topological neighbours' information so that one manipulator acts to fulfil the task, whereas the others do not move. Furthermore, the proposed Dk-WTA scheme is validated by simulations and experiments based on multiple manipulators. However, the application scenario in this article is relatively simple, and the communication topology used in this article is restricted to undirected and fixed graphs, which do not take into account the complex and changeable communication environments in reality. Therefore, applying the proposed scheme to more complex embodied multi-agent systems [38, 39] and extending it to directed topologies [40] and switching topologies [41] are future research directions.

Funding

This work was supported by the National Natural Science Foundation of China (Grant 62503208).

Conflicts of Interest

The authors declare no conflicts of interest.

Data Availability Statement

The data that support the findings of this study are available on request from the corresponding author upon reasonable request.

References

1. P. T. Jiang, C. B. Zhang, Q. Hou, M. M. Cheng, and Y. W. LayerCAM, "Exploring Hierarchical Class Activation Maps for Localization," *IEEE Transactions on Image Processing* 30 (2021): 5875–5888, https://doi.org/10.1109/tip.2021.3089943.

2. D. B. Sam, S. V. Peri, M. N. Sundararaman, A. Kamath, and R. V. Babu, "Locate, Size, and Count: Accurately Resolving People in Dense Crowds via Detection," *IEEE Transactions on Pattern Analysis and Machine Intelligence* 43, no. 8 (2021): 2739–2751, https://doi.org/10.1109/TPAMI.2020.2974830.

3. S. Li, L. Jin, and S. Li, "Modeling and Analysis of Competitive Behavior in Social Systems," *IEEE Transactions on Computational Social Systems* 10, no. 3 (2023): 1347–1355, https://doi.org/10.1109/tcss.2022.3163799.

4. S. Liang, B. Peng, P. Stanimirović, and L. Jin, "Design, Analysis, and Application of Projected k-Winner-Take-All Network," *Information Sciences* 621 (2023): 74–87, https://doi.org/10.1016/j.ins.2022.11.090.

5. E. Majani, R. Erlanson, and Y. Abu-Mostafa, "On the k-Winners-Take-All Network," in *Advances in Neural Information Processing System*, (1989), 634–642.

6. B. D. Calvert and C. A. Marinov, "Another k-Winner-Take-All Analog Neural Network," *IEEE Transactions on Neural Networks* 11, no. 4 (2000): 829–838, https://doi.org/10.1109/72.857764.

7. P. V. Tymoshchuk, "A Discrete-Time Dynamic k-Winners-Take-All Neural Circuit," *Neurocomputing* 72, no. 13–15 (2009): 3191–3202, https://doi.org/10.1016/j.neucom.2009.03.001.

8. P. V. Tymoshchuk and D. C. Wunsch, "Design of a k-Winners-Take-All Model With a Binary Spike Train," *IEEE Transactions on Cybernetics* 49, no. 8 (2019): 3131–3140, https://doi.org/10.1109/tcyb.2018.2839691.

9. S. Liu and J. Wang, "A Simplified Dual Neural Network for Quadratic Programming With Its kWTA Application," *IEEE Transactions on Neural Networks* 17, no. 6 (2006): 1500–1510, https://doi.org/10.1109/TNN.2006.881046.

10. X. Hu and J. Wang, "An Improved Dual Neural Network for Solving a Class of Quadratic Programming Problems and Its k-Winners-Take-All Application," *IEEE Transactions on Neural Networks* 19, no. 12 (2008): 2022–2031, https://doi.org/10.1109/tnn.2008.2003287.

11. R. Feng, C.-S. Leung, and J. Sum, "Robustness Analysis on Dual Neural Network-Based K WTA With Input Noise," *IEEE Transactions on Neural Networks and Learning Systems* 29, no. 4 (2018): 1082–1094, https://doi.org/10.1109/tnnls.2016.2645602.

12. J. Sum, C.-S. Leung, and K. I.-J. Ho, "On Wang K WTA With Input Noise, Output Node Stochastic, and Recurrent State Noise," *IEEE Transactions on Neural Networks and Learning Systems* 29, no. 9 (2018): 4212–4222, https://doi.org/10.1109/tnnls.2017.2759905.

13. X. Zhao, Q. Zong, B. Tian, and M. You, "Finite-Time Dynamic Allocation and Control in Multiagent Coordination for Target Tracking," *IEEE Transactions on Cybernetics* 52, no. 3 (2022): 1872–1880, https://doi.org/10.1109/tcyb.2020.2998152.

14. Z. Cui, X. Gu, and N. Tan, "Distributed Formation Control for Heterogeneous Robot Systems Based on Competitive Mechanism," *CAAI Transactions on Intelligence Technology* 11, no. 1 (2026): 190–204, https://doi.org/10.1049/cit2.70081.

15. M. Liu, Y. Li, Y. Chen, Y. Qi, and L. Jin, "A Distributed Competitive and Collaborative Coordination for Multirobot Systems," *IEEE Transactions on Mobile Computing* 23, no. 12 (2024): 11436–11448, https://doi.org/10.1109/tmc.2024.3397242.

16. C. Lin, Y. Zhang, and S. Li, "Distributed k-Winners-Take-All With Privacy Protection: Method and Hardware Experiments," *IEEE Transactions on Industrial Electronics* (2026): 1–11, https://doi.org/10.1109/TIE.2026.3675190.

17. R. A. Freeman, P. Yang, and K. M. Lynch, "Stability and Convergence Properties of Dynamic Average Consensus Estimators," in *Proceedings of the IEEE Conference on Decision and Control*, (2006), 338–343.

18. L. Jin and S. Li, "Distributed Task Allocation of Multiple Robots: A Control Perspective," *IEEE Transactions on Systems, Man, and Cybernetics: Systems* 48, no. 5 (2018): 693–701, https://doi.org/10.1109/tsmc.2016.2627579.

19. Y. Zhang, S. Li, B. Xu, and Y. Yang, "Analysis and Design of a Distributed k-Winners-Take-All Model," *Automatica* 115 (2020): 108868, https://doi.org/10.1016/j.automatica.2020.108868.

20. X. Wang, S. Yang, Z. Guo, and T. Huang, "Distributed k-Winners-Take-All via Multiple Neural Networks With Inertia," *Neural Networks* 151 (2022): 385–397, https://doi.org/10.1016/j.neunet.2022.04.005.

21. Y. Kong, C. Zhang, J. Zhou, and J. Zhou, "Comprehensive Understanding of a Distributed k-WTA Strategy in a Competitive Behavior," *Communications in Nonlinear Science and Numerical Simulation* 125 (2023): 107382, https://doi.org/10.1016/j.cnsns.2023.107382.

22. Z. Zeng, J. Wang, and X. Liao, "Global Exponential Stability of a General Class of Recurrent Neural Networks With Time-Varying Delays," *IEEE Transactions on Circuits and Systems I* 50, no. 10 (2003): 1353–1358, https://doi.org/10.1109/TCSI.2003.817760.

23. Y. Zhang, S. Li, J. Weng, and B. Liao, "GNN Model for Time-Varying Matrix Inversion With Robust Finite-Time Convergence," *IEEE Transactions on Neural Networks and Learning Systems* 35, no. 1 (2024): 559–569, https://doi.org/10.1109/tnnls.2022.3175899.

24. Y. Zhang, B. Liao, and G. Geng, "GNN Model With Robust Finite-Time Convergence for Time-Varying Systems of Linear Equations," *IEEE Transactions on Systems, Man, and Cybernetics: Systems* 54, no. 8 (2024): 4786–4797, https://doi.org/10.1109/tsmc.2024.3387023.

25. Z. Xie, J. Zhou, J. Zhao, and L. Jin, "Sparsity-Infused Position and Orientation Control for Redundant Manipulators," *IEEE Transactions on Systems, Man, and Cybernetics: Systems* 56, no. 7 (2026): 4336–4346, https://doi.org/10.1109/TSMC.2026.3678998.

26. J. Liu, Z. Jiang, X. Xu, W. Li, M. Liu, and H. Liu, "Multi-Robot Collaborative Complex Indoor Scene Segmentation via Multiplex Interactive Learning," *CAAI Transactions on Intelligence Technology* 10, no. 6 (2025): 1646–1660, https://doi.org/10.1049/cit2.70066.

27. C. Hua, X. Cao, J. Li, and S. Li, "Fixed-Time Zeroing Neural Dynamics for Adaptive Coordination of Multi-Agent Systems," *CAAI Transactions on Intelligence Technology* 20, no. 8 (2024): 9918–9927, https://doi.org/10.1049/cit2.70089.

28. J. Tang, Z. Xie, and L. Jin, "Collision Avoidance MPC for IBVS of Redundant Manipulators," *IEEE Transactions on Automation Science and Engineering* 23, no. 5 (2026): 9571–9580, https://doi.org/10.1109/TASE.2026.3692473.

29. M. Liu and M. Shang, "On RNN-Based k-WTA Models With Time-Dependent Inputs," *IEEE/CAA Journal of Automatica Sinica* 9, no. 11 (2022): 2034–2036, https://doi.org/10.1109/jas.2022.105932.

30. L. Jin, Y. Chen, and M. Liu, "A Noise-Tolerant k-WTA Model With Its Application on Multirobot System," *IEEE Transactions on Industrial Informatics* 20, no. 3 (2024): 3574–3584, https://doi.org/10.1109/tii.2023.3308330.

31. Y. Zhang, S. Li, and J. Weng, "Distributed k-Winners-Take-All Network: An Optimization Perspective," *IEEE Transactions on Cybernetics* 53, no. 8 (2023): 5069–5081, https://doi.org/10.1109/tcyb.2022.3170236.

32. H. Huang, L. Jin, and Z. Zeng, "A Momentum Recurrent Neural Network for Sparse Motion Planning of Redundant Manipulators With Majorization-Minimization," *IEEE Transactions on Industrial Electronics* 72, no. 12 (2025): 13532–13541, https://doi.org/10.1109/tie.2025.3566731.

33. Y. Zhang and S. Li, "Kinematic Control of Serial Manipulators Under False Data Injection Attack," *IEEE/CAA Journal of Automatica Sinica* 10, no. 4 (2023): 1009–1019, https://doi.org/10.1109/jas.2023.123132.

34. Z. Xie, X. Wu, and L. Jin, "Integral-Enhanced Hierarchical Control for Redundant Manipulators With Unknown Kinematics," *IEEE Transactions on Automation Science and Engineering* 23, no. 4 (2026): 6426–6436, https://doi.org/10.1109/TASE.2026.3671955.

35. L. Wei, L. Jin, and X. Luo, "Noise-Suppressing Neural Dynamics for Time-Dependent Constrained Nonlinear Optimization With Applications," *IEEE Transactions on Systems, Man, and Cybernetics: Systems* 52, no. 10 (2022): 6139–6150, https://doi.org/10.1109/tsmc.2021.3138550.

36. Z. Zeng, J. Wang, and X. Liao, "Stability Analysis of Delayed Cellular Neural Networks Described Using Cloning Templates," *IEEE Transactions on Circuits and Systems I* 51, no. 11 (2004): 2313–2324, https://doi.org/10.1109/tcsi.2004.836855.

37. Y. Zhang, B. Mu, and H. Zheng, "Link Between and Comparison and Combination of Zhang Neural Network and Quasi-Newton BFGS Method for Time-Varying Quadratic Minimization," *IEEE Transactions on Cybernetics* 43, no. 2 (2023): 490–503, https://doi.org/10.1109/TSMCB.2012.2210038.

38. Y. Peng, X. Zhang, H. Xie, and X. Xu, "Hybrid Distributed and Decentralised Reinforcement Learning for Formation Control of Multi-Robots With Obstacle Avoidance," *CAAI Transactions on Intelligence Technology* 10, no. 5 (2025): 1337–1349, https://doi.org/10.1049/cit2.70002.

39. J. Li, J. Wang, H. Gao, X. Luo, and C. L. P. Chen, "Dynamic Neural-Model-Based Predictive Control for Autonomous Wheel-Legged Robot System," *CAAI Transactions on Intelligence Technology* 11, no. 1 (2026): 83–97, https://doi.org/10.1049/cit2.70091.

40. Y. Zhou, H. Hu, W. Ding, K. Gao, D. Li, and F. Gao, "Cooperative Distributed Predictive Control for Smart Injection Molding Systems With One-Tap Memory," *IEEE Transactions on Industrial Informatics* 20, no. 6 (2024): 8850–8860, https://doi.org/10.1109/tii.2024.3378838.

41. M. Z. Shahabadi, H. Atrianfar, G. B. Gharehpetian, and A. Yazdani, "Distributed Self-Triggered Control of Islanded Microgrids Under Switching Communication Topologies," *IEEE Transactions on Industrial Informatics* 20, no. 12 (2024): 13904–13915, https://doi.org/10.1109/tii.2024.3438235.